iScience, Volume *26*

Supplemental information

Piezo1 induces endothelial responses to shear stress via soluble adenylyl Cyclase-IP_3R2 circuit

Dianicha Santana Nunez, Asrar B. Malik, Quinn Lee, Sang Joon Ahn, Arnold Coctecon-Murillo, Dana Lazarko, Irena Levitan, Dolly Mehta, and Yulia A. Komarova

Supplemental Figures

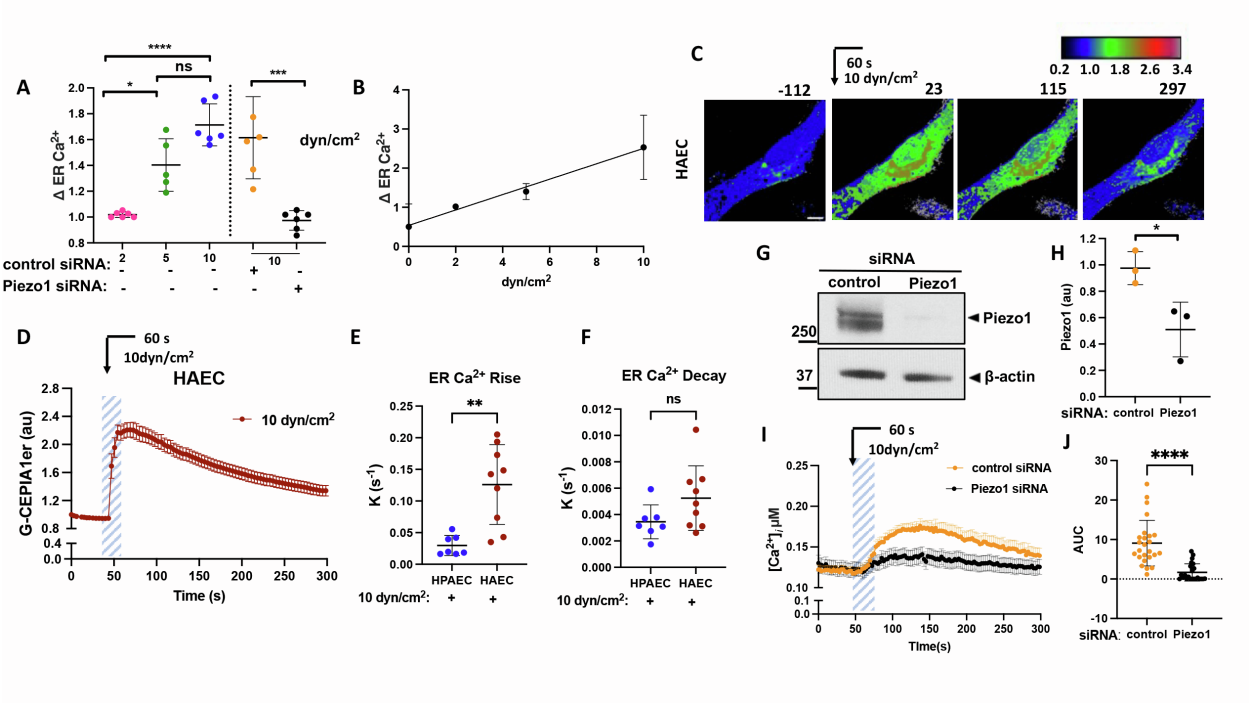

Figure S1. Activation of Piezo1 by laminar shear stress induces transient mobilization of Ca^{2+} into the ER lumen. Supplemental data related to Figure 1.

A. Peak changes in $[Ca^{2+}]_{ER}$ calculated from data in **1B;** n=5-7 cell per group from 3 independent experiments; left; mean ± SD; *, $p < 0.05$; ****, $p < 0.0001$, ANOVA with Tukey's post hoc test; right, ***, $p < 0.001$, Student's *t* test**.**

B. Linear regression modeling of data in **A** indicating that Ca^{2+} entry to the ER is proportional to the shear stress level.

C. Live-cell images of G-CEPIA1er in HAE monolayers before and after application of 10 dyn/cm^2 fluid shear for 60 seconds; color-coding is shown in the heat map; times in seconds; scale bar, 10 µm.

D. Time-dependent changes of $[Ca^{2+}]_{ER}$ in HAE monolayers before and after application of 10 dyn/cm^2 shear stress for 60 seconds (highlighted area); n=9 cells from 2 independent experiments; mean ± SEM.

E. Rate constants of ER Ca^{2+} rise calculated from data in **D** compared to data in Fig **1C** for 10 dyn/cm^2 shear stress; mean ± SD; **, $p < 0.01$, Student's *t* test.

F. Rate constants of ER Ca^{2+} decay calculated from data in **D** compared to data in Fig **1C** for 10 dyn/cm^2 shear stress; mean ± SD; ns, not significant, Student's *t* test.

G. Western blot analysis of Piezo1 in endothelial cells monolayer pre-treated with control and Piezo1 siRNA; β-actin, loading control.

H. Quantification of data in **H**; data are presented as 3 biological replicates from 3 independent experiments; mean ± SD; *, $p < 0.05$, Student's *t* test.

I. Time-dependent changes of $[Ca^{2+}]_i$ before and after application of 10 dyn/cm^2 shear stress for 60 seconds (highlighted area) in endothelial monolayers pre-treated with control or Piezo1 siRNA; n=24-25 cells per group from 2 independent experiments; mean ± SEM.

J. Changes of $[Ca^{2+}]_i$ within the first 300s (area under the curve) after application of shear stress for 60 seconds calculated from data in **I**; mean ± SD; ****, $p < 0.0001$, Student's *t* test**.**

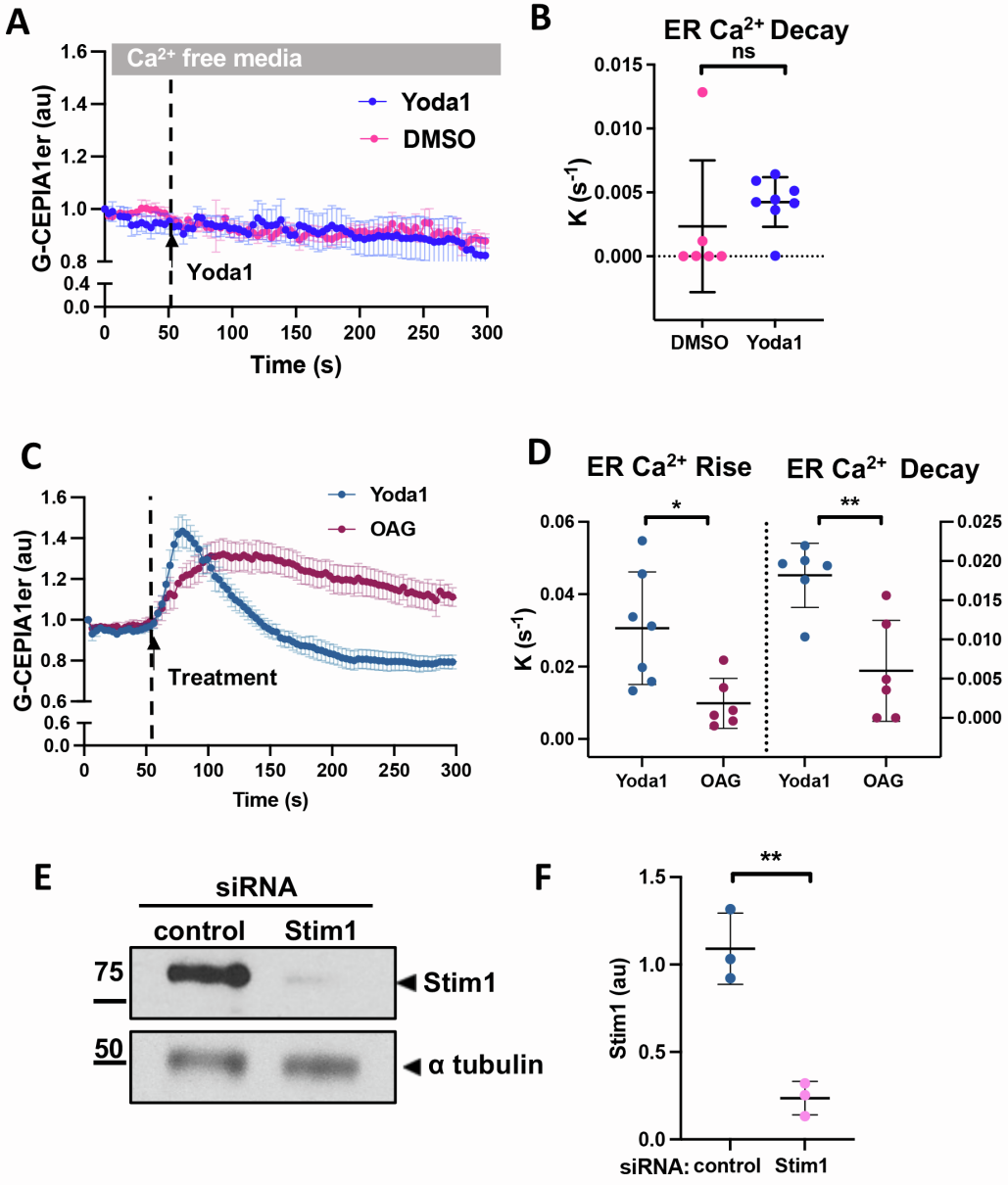
A
Ca2+ free media
Yoda1
DMSO
G-CEPIA1er (au)
Yoda1
Time (s)
B
ER Ca2+ Decay
ns
K (s-1)
DMSO
Yoda1
C
Yoda1
OAG
G-CEPIA1er (au)
Treatment
Time (s)
D
ER Ca2+ Rise
ER Ca2+ Decay
*
**
K (s-1)
Yoda1
OAG
Yoda1
OAG
E
siRNA
control
Stim1
75
Stim1
50
α tubulin
F
**
Stim1 (au)
siRNA: control
Stim1

Figure S2. Activation of Piezo1 induces rapid mobilization of Ca^{2+} into the ER. Supplemental data related to Figure 2.

A. Time-dependent changes of $[Ca^{2+}]_{ER}$ in endothelial monolayers stimulated with Yoda1 (arrow) in nominal Ca^{2+} free medium; n= 6-8 cells per group from 3 independent experiments.

B. The rate constants of ER Ca^{2+} decay calculated from data in **A**; mean ± SD; ns, Student's *t* test.

C. Time-dependent changes of $[Ca^{2+}]_{ER}$ in endothelial monolayers stimulated with Yoda1 or OAG (arrow); n= 6-7 cells per group from 3 independent experiments; mean ± SEM.

D. The rate constants of ER Ca^{2+} rise and decay calculated from data in **C**; mean ± SD.; *, $p < 0.05$, Student's *t* test; **, $p < 0.01$, Student's *t* test.

E. Western blot analysis of STIM1 in endothelial cells pre-treated with control or STIM1 siRNA; α-tubulin, loading control.

F. Quantification of data in **F**; data are presented as 3 biological replicates from 3 independent experiments **, $p < 0.01$, Student's *t* test.

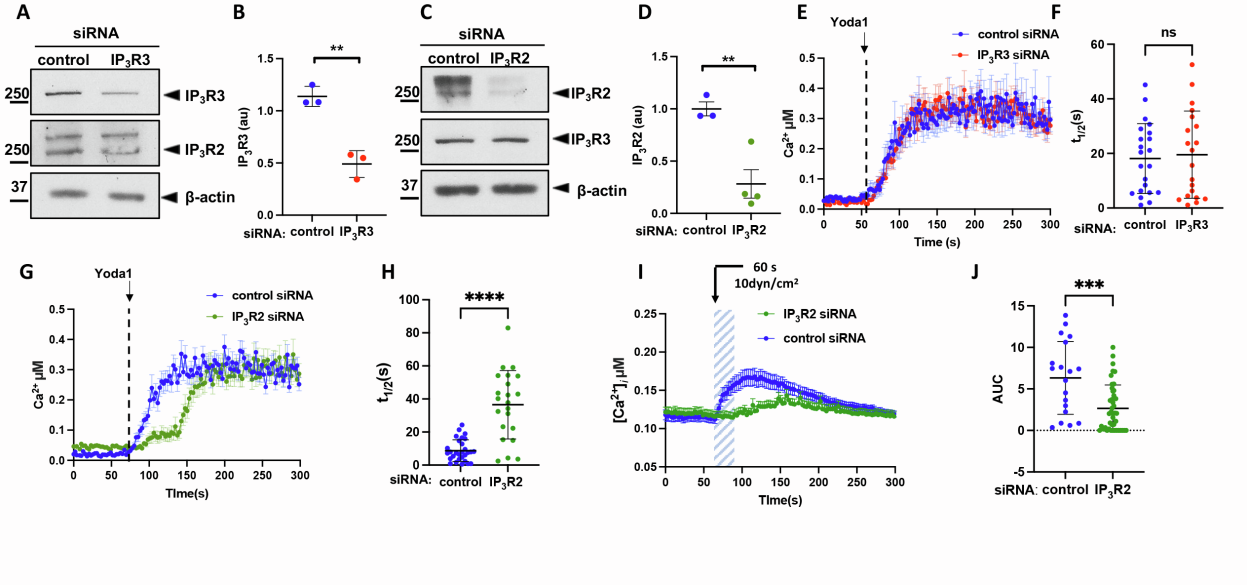

Figure S3. Depletion of IP$_3$R2 but not IP$_3$R3 alleviate Piezo1 induced increase in cytosolic *[Ca^{2+}]$_i$*. Supplemental data related to Figure 3.

A. Western blot analysis of IP$_3$R2 and IP$_3$R3 protein expressions in endothelial cells pre-treated with control or IP$_3$R3 siRNA; β-actin, loading control. Depletion of IP$_3$R3 did not alter IP$_3$R2 protein level.

B. Quantification of data in **A**; data are presented as 3 biological replicates from 3 independent experiments; **, $p < 0.01$, Student's *t* test.

C. Western blot analysis of IP$_3$R2 and IP$_3$R3 protein expressions in endothelial cells pre-treated with control and IP$_3$R2 siRNA; β-actin, loading control. Depletion of IP$_3$R2 did not alter IP$_3$R3 protein level.

D. Quantification of data in **C**; data are presented as 4 biological replicates from 4 independent experiments; **, $p < 0.01$, Student's *t* test.

E. Time-dependent changes of *[Ca^{2+}]$_i$* upon activation of Piezo1 with Yoda1 (arrow) in endothelial monolayers pre-treated with control or IP$_3$R3 siRNA; n=18-21 cells per group from 3 independent experiments; mean ± SEM.

F. Half-time ($t_{½}$) of cytosolic $[Ca^{2+}]_i$ increase from data in **E**.; ns, not significant, Student's *t* test.

G. Time-dependent changes of cytosolic $[Ca^{2+}]_i$ upon activation of Piezo1 with Yoda1 (arrow) in endothelial monolayers pre-treated with control or IP_3R2 siRNA; n=22-29 cells per group from 3 independent experiments; mean ± SEM.

H. Half-time ($t_{½}$) of $[Ca^{2+}]_i$ increase from data in **G** ; ****, p <0.0001, Student's *t* test**.**

I. Time-dependent changes of $[Ca^{2+}]_i$ before and after application of 10 dyn/cm^2 shear stress for 60 seconds (highlighted area) in endothelial monolayers pre-treated with control or IP_3R2 siRNA; n=19-35 cells per group from 3 independent experiments; mean ± SEM.

J. Changes in $[Ca^{2+}]_i$ within the first 300s (area under the curve) after application of shear stress for 60 seconds calculated from data in **I**; mean ± SD; ***, $p < 0.001$, Student's *t* test**.**

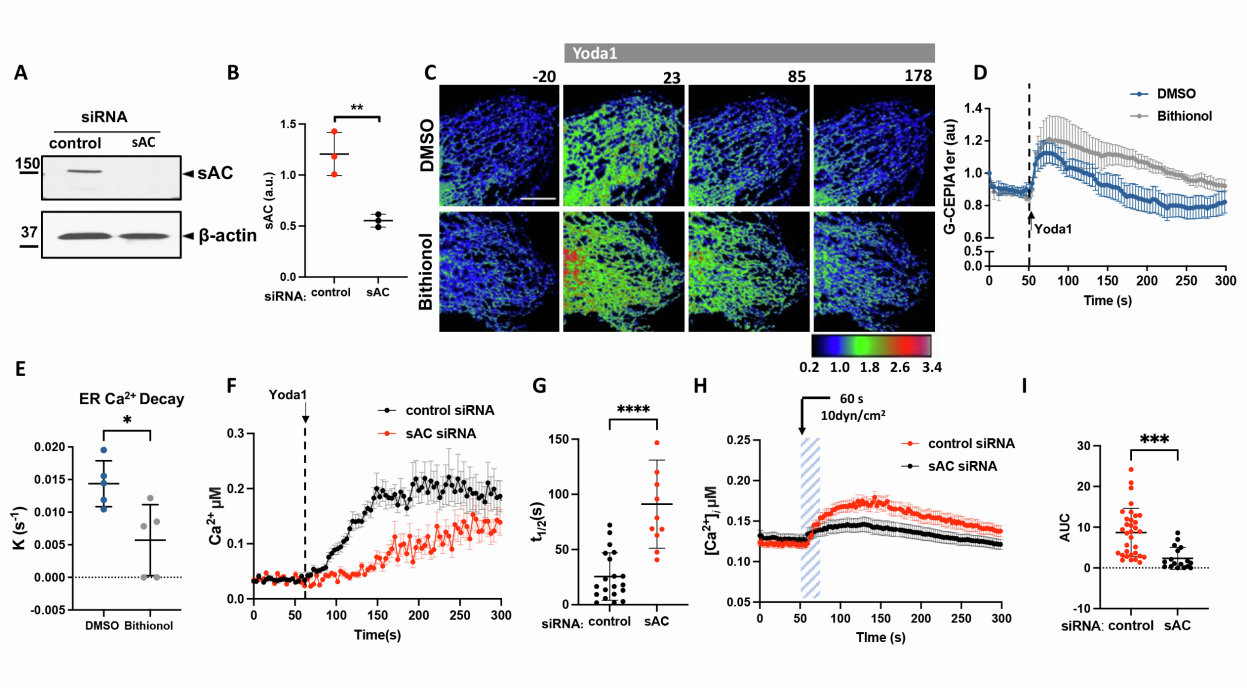

Figure S4. Genetic and pharmacological ablation of sAC impairs Piezo1-mediated ER Ca^{2+} release and an increase in $[Ca^{2+}]_i$. Supplemental data related to Figure 4.

A. Western blot analysis of sAC protein in endothelial monolayers pre-treated with control and sAC siRNA; β-actin, loading control.

B. Quantification of data in **A**; data are presented as 3 biological replicates from 3 independent experiments; **, $p < 0.01$, Student's *t* test.

C. Live-cell images of G-CEPIA1er before and after activation of Piezo1 with Yoda1 in endothelial monolayers pretreated vehicle (DMSO) or sAC inhibitor bithionol; color-coding as in **1A**; time in seconds; scale bar, 10µm.

D. Time course of $[Ca^{2+}]_{ER}$ in **C**; n=6 cells per group from 3 independent experiments; mean ± SEM.

E. The rate constants of ER Ca^{2+} decay calculated from data in **D**; *, p <0.05, Student's *t* test

F. Time-dependent changes of cytosolic $[Ca^{2+}]_i$ upon activation of Piezo1 with Yoda1 (arrow) in endothelial monolayers pre-treated with control or sAC siRNA; n=10-19 cells per group from 3 independent experiments; mean ± SEM.

G. Half time ($t_{½}$) of $[Ca^{2+}]_i$ increase from data in **F**; ****, p <0.0001, Student's *t* test.

H. Time-dependent changes of cytosolic $[Ca^{2+}]_i$ before and after application of 10 dyn/cm^2 shear stress for 60 seconds (highlighted area) in endothelial monolayers pre-treated with control or sAC siRNA; n=17-28 cells per group from 3 independent experiments; mean ± SEM.

I. Changes in $[Ca^{2+}]_i$ within the first 300s (area under the curve) of shear application; calculated from data in **H**; mean ± SD; ***, $p < 0.001$, Student's *t* test**.**

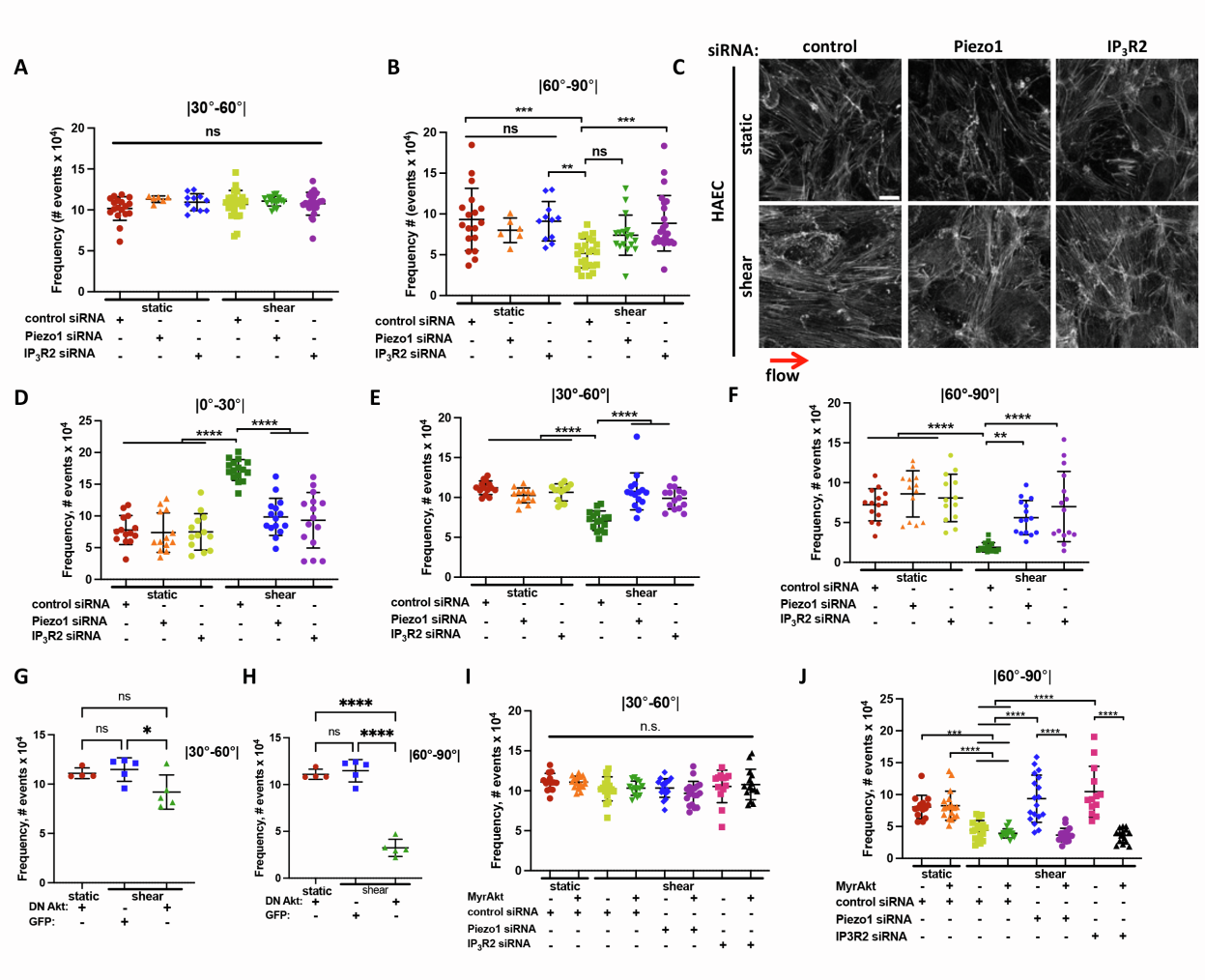

Figure S5. Depletion of Piezo1 or IP$_3$R2 prevents activation of Akt and consequent EC alignment in the direction of flow. Supplemental data related to Figure 5 and 6.

A-B. Frequency of F-actin distribution within 30-60° (**A**) and a 60-90° (**B**) relative to the direction of flow; groups as in **Fig 5B;** n= 6-15 field per condition, from 2-4 independent experiment on static group and 17-24 fields per condition from 4 independent experiments on shear group; **, $p < 0.01$; ***, $p < 0.001$; ns, not significant, ANOVA with Tukey's post hoc test.

C. Representative images of F-actin in HAE monolayers depleted of indicated proteins and grown under static or 10 dyn/cm^2 laminar shear flow conditions for 24 hours; arrow indicates direction of flow; scale bar 20 μm.

D-F. Frequency of F-actin distribution within 0-30° (**D**), 30-60° (**E**) and 60-90° (**F**) relative to the direction of flow in HAE monolayers in C; n= 14-15 field per condition, from 3 independent experiments; mean ± SD; **, $p < 0.01$, ****, $p < 0.0001$, ANOVA with Tukey's post hoc test.

G-H. Frequency of F-actin distribution within 30-60° (**G**) and 60-90° (**H**) relative to the direction of flow of cells in **Fig 6A**; n=5-10 fields per condition from 2 independent experiments; *, $p < 0.05$; ****, $p < 0.0001$, ANOVA with Tukey's post hoc test

I-J Frequency of F-actin distribution within 30-60° (**I**) and a 60-90° (**J**) relative to the direction of flow; groups as in **Fig 6C**; n=14 -18 fields per condition across 3 independent experiments; ***, $p < 0.001$; ****, $p < 0.0001$; ns, not significant, ANOVA with Tukey's post hoc test.